ResearchGate

See discussions, stats, and author profiles for this publication at: https://www.researchgate.net/publication/234008576

Charge Transport in a Highly Phosphorescent Iridium(III) Complex–Cored Dendrimer with Double Dendrons

ARTICLE *in* ADVANCED FUNCTIONAL MATERIALS · JANUARY 2012

Impact Factor: 11.81 · DOI: 10.1002/adfm.201101727

CITATIONS
10

READS
28

5 AUTHORS, INCLUDING:

Salvatore Gambino
Università del Salento
26 PUBLICATIONS **195** CITATIONS
SEE PROFILE

Shih-Chun Lo
University of Queensland
76 PUBLICATIONS **2,544** CITATIONS
SEE PROFILE

Ifor David William Samuel
University of St Andrews
448 PUBLICATIONS **11,345** CITATIONS
SEE PROFILE

All in-text references underlined in blue are linked to publications on ResearchGate, letting you access and read them immediately.

Available from: Salvatore Gambino
Retrieved on: 27 January 2016

Charge Transport in a Highly Phosphorescent Iridium(III) Complex-Cored Dendrimer with Double Dendrons

Salvatore Gambino, Shih-Chun Lo, Zehua Liu, Paul L. Burn, and Ifor D. W. Samuel**

The charge transporting properties of a phosphorescent iridium(III) complex-cored dendrimer, with two dendrons attached to each ligand of the core are reported. The results show that the high photoluminescence quantum yield of this material is obtained without compromising charge transport. The hole mobility values are reported over a wide range of temperatures and electric fields using the charge-generation layer time-of-flight technique. The results are analysed using the Gaussian disorder model (GDM), the correlated disorder model, the polaronic correlated disorder model, and the short-range correlated Gaussian disorder model. It is found that the GDM model gives the most comprehensive description of hole transport in this material. In spite of its larger size, the hole mobility of the doubly dendronised material compares favourably with that of a smaller singly dendronised material, and its spherical shape leads to low energetic disorder and clearly non-dispersive charge transport. This shows how molecular shape can be used to combine favourable photoluminescence and charge-transporting properties.

1. Introduction

The development of light-emitting materials for organic light-emitting diodes has led to a range of strategies for controlling intermolecular interactions. For organic light-emitting diodes (OLEDs) it is important that the materials have a high photoluminescence quantum yield (PLQY) but still have sufficient charge mobility to avoid high driving voltages. There is often a trade-off between efficiency of light emission and charge transport; namely it is advantageous to space the luminescent chromophores apart to reduce intermolecular interactions that can quench the luminescence,[1–5] but as the luminescent chromophore is normally also responsible for charge transport, a large separation would be detrimental to charge mobility.[6] Hence the challenge for materials development is to have good photophysical properties without sacrificing charge transporting properties.[7–10]

We explore this issue of solid-state inter-chromophore interactions using light-emitting conjugated dendrimers, which are well-defined soluble organic semiconductors.[11–13] Light-emitting dendrimers generally comprise a light-emitting core, to which one or more dendrons (branched structures) are attached. Surface groups are often used at the distal ends of the dendrons to provide solubility and processability. Light-emitting dendrimers allow good control over intermolecular interactions, giving a powerful way of exploring their role in the charge transport and photophysics of organic semiconductors. We have shown that the degree of interaction between chromophores can also be manipulated by dendrimer generation and have investigated the effect this has on the material properties.[14,15] We have also demonstrated that the dendron type can have a dramatic effect on the optoelectronic properties of the materials.[5,8,13,16]

Another strategy for controlling the intermolecular interactions is increasing the number of dendrons attached to the core. In our work on phosphorescent *fac*-tris(2-phenylpyridyl) iridium(III) complex-cored dendrimers we have prepared three generations of materials that contain a single biphenyl dendron with 2-ethylhexyloxy surface groups attached to each of the ligands.[17,18] However, with these mono-dendronised (one dendron per ligand) materials, the dendrons fan out from the core in one direction giving the shape of a shuttlecock with the complex at its base due to the octahedral geometry. This means that for these mono-dendronised materials one face of the opto-electronic core chromophore is open to intermolecular interactions. This can be overcome by making the so-called "double-dendron" materials, which have two dendrons attached to each ligand of the core. **Figure 1** shows the space filling models for a first generation mono- (IrG1) and doubly dendronised (DDIrG1) iridium(III) complex-cored dendrimer. The use of the doubly dendronised material has enabled very efficient film photoluminescence (PLQY 81%)[19] and electroluminescence (13.6% external quantum efficiency at 110 cd/m^2) to be

Dr. S. Gambino, Prof. I. D. W. Samuel
Organic Semiconductor Centre
SUPA, School of Physics and Astronomy
University of St Andrews, North Haugh
St Andrews KY16 9SS, UK
E-mail: idws@st-andrews.ac.uk
Dr. S.-C. Lo, Prof. P. L. Burn
Centre for Organic Photonics and Electronics
The University of Queensland, Chemistry Building
Queensland 4072, Australia
E-mail: paul.burn@uq.edu.au
Dr. Z. Liu
Department of Chemistry
Chemistry Research Laboratory
University of Oxford
Mansfield Road, Oxford, OX1 3TA, UK

DOI: 10.1002/adfm.201101727

© 2012 WILEY-VCH Verlag GmbH & Co. KGaA, Weinheim

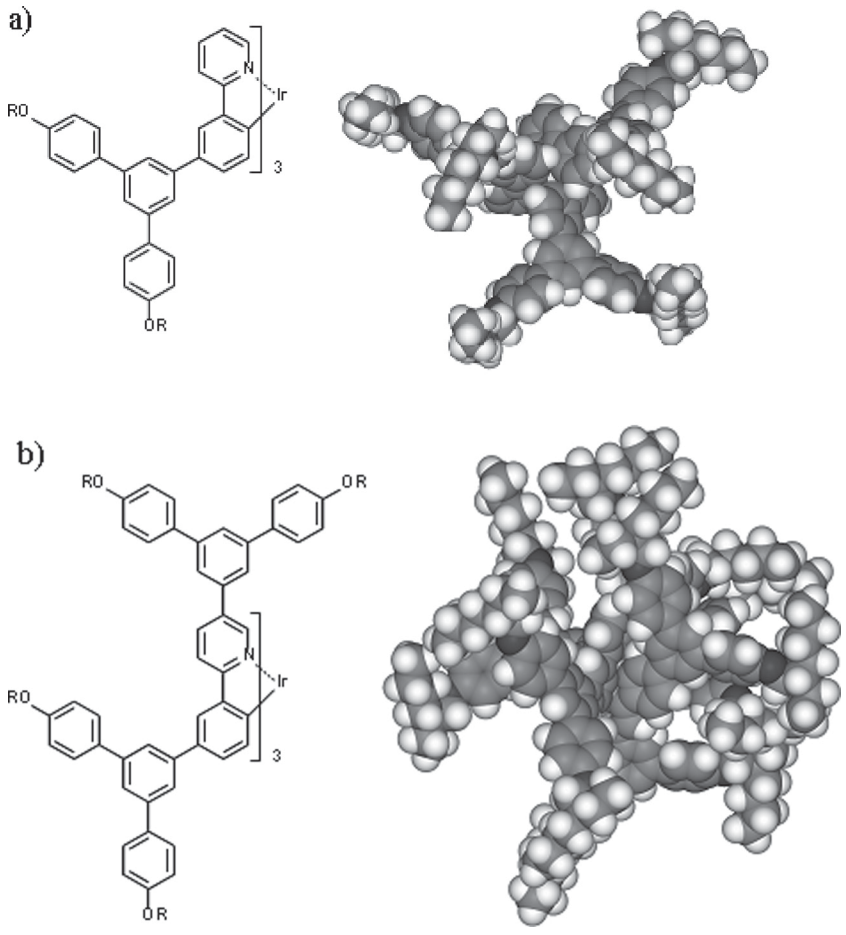

Figure 1. a) Mono-dendronised (IrG1) and b) doubly dendronised (DDIrG1) *fac*-tris(2-phenylpyridyl)iridium(III) complex cored-dendrimers with first generation biphenyl dendrons and 2-ethylhexyloxy surface groups. R = 2-ethylhexyl.

obtained from neat films of a first-generation material.[19,20] In contrast the mono-dendronised IrG1 has a solid state PLQY of 65%,[19] showing that a double-dendron structure is more effective in controlling the intermolecular interactions that affect the luminescence efficiency. However, the question arises as to how this protection of the luminescent core affects the charge transport in neat films of the doubly dendronised material and whether adequate charge transport properties can be combined with highly efficient luminescence.

In this paper we explore the effect that the double dendron structure has on the charge transport properties in order to show how good luminescence quantum yield and sufficient charge transport can be achieved in the same material. We explore this by measuring the temperature and field dependence of the hole mobility, using the charge-generation layer time-of-flight (TOF) technique (**Figure 2** inset), for the doubly dendronised iridium(III) complex. Furthermore we analyze the experimental results within the Gaussian disorder model (GDM),[21] correlated disorder model (CDM),[22] polaronic correlated disorder model (polaronic CDM),[23] and short range correlated Gaussian disorder model (short CDM).[24]

2. Results

Figure 3 shows the hole photocurrent transient on linear and log-log scales for a DDIrG1 film, at room temperature for an applied electric field, $E = 2.5 \times 10^5$ Vcm^{-1}. The plot shows an initial spike followed by a clear constant-current plateau. This corresponds to non-dispersive hole transport with a time-independent drift velocity. The subsequent drop in the current is caused by the holes reaching the ITO electrode, where they are discharged. The carrier transit time (t_{tr}) was evaluated from the intersection point of the asymptotes to the plateau and to the long tail, $t_{tr} = 0.07$ ms. The transit time of 0.07 ms corresponds to a mobility of 2.2×10^{-6} cm^2 V^{-1} s^{-1}. The TOF measurements give the hole mobility in the direction perpendicular to the substrate, and we have studied its field dependence, as shown in **Figure 4**. As the electric field is increased from 1.2×10^5 to 5×10^5 V cm^{-1}, the hole mobility increases from 1.1×10^{-6} to 8.3×10^{-6} cm^2 V^{-1} s^{-1} at room temperature. In order to compare the effect of having two dendrons attached to each ligand on the charge mobility the room temperature hole mobility of the singly dendronised dendrimer (IrG1) was also measured, with the results plotted in Figure 4 for a direct comparison. It is clear that both materials have the same field dependence and similar mobility values, which is surprising given that the core, which is responsible for the hole transport, of the DDIrG1 is encapsulated by the dendrons and so might be expected to have lower charge mobility.

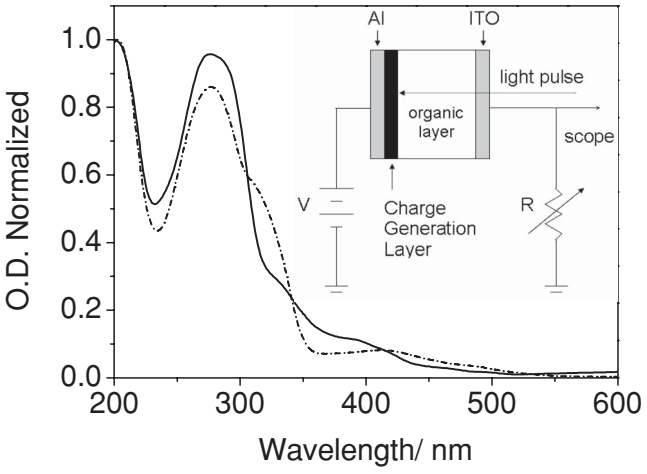

Figure 2. Absorption spectra of the first generation mono- (solid line) and doubly (dotted line) dendronised iridium(III) complex-cored dendrimer (i.e., IrG1 and DDIrG1, respectively) thin films. Charge-generation layer TOF set-up schematic (inset).

© 2012 WILEY-VCH Verlag GmbH & Co. KGaA, Weinheim

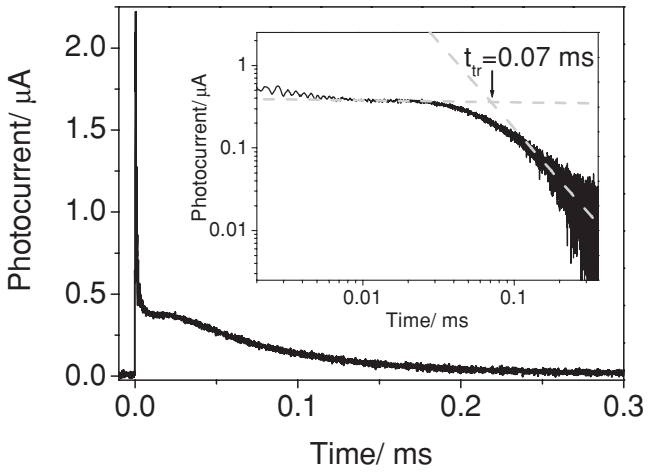

Figure 3. Hole photocurrent transient on linear and log-log scales (inset) for a DDIrG1 film, at room temperature for an applied electric field $E = 2.5 \times 10^5$ Vcm^{-1}.

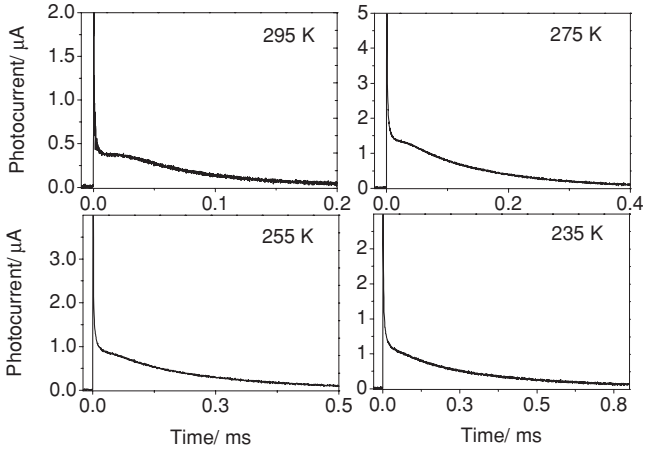

Figure 5. Hole photocurrent transients at an electric field of $E = 2.5 \times 10^5$ Vcm^{-1}. Measurements were performed in vacuum and in a temperature range of 235–295 K.

To learn more about the charge-transport mechanism, temperature-dependent measurements were performed on DDIrG1. **Figure 5** shows the hole photocurrent transients on a linear scale from 295 K down to 235 K for an applied electric field $E = 2.5 \times 10^5$ V cm^{-1}. As the temperature is decreased, the photocurrent plateau becomes less distinct and starts to disappear below 275 K. **Figure 6** shows DDIrG1 hole mobility as a function of field for temperatures from 215 K to 335 K in intervals of 20 K.

2.1. Gaussian Disorder Model

We first analysed the field and temperature dependent mobility data on the basis of Equation 1 to determine σ, μ_0, Σ and C:[21]

$$\mu(T, E) = \mu_0 \exp\left[-\left(\tfrac{2}{3}\hat{\sigma}\right)^2\right] \exp\left[C\left(\hat{\sigma}^2 - \Sigma^2\right) E^{1/2}\right] \Sigma \geq 1.5$$
$$\mu(T, E) = \mu_0 \exp\left[-\left(\tfrac{2}{3}\hat{\sigma}\right)^2\right] \exp\left[C\left(\hat{\sigma}^2 - 2.25\right) E^{1/2}\right] \Sigma < 1.5 \quad (1)$$

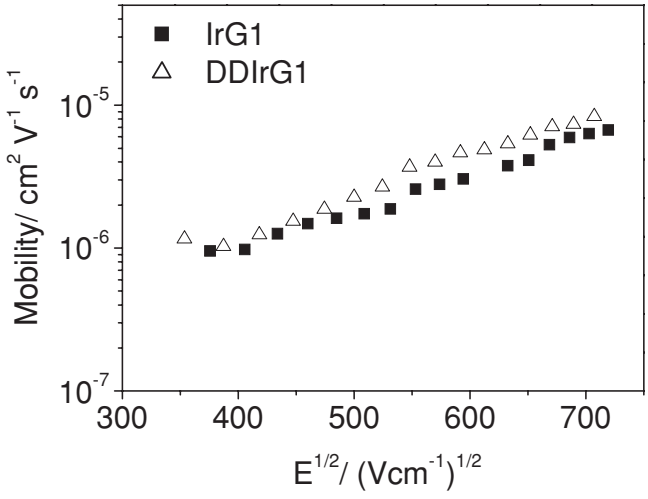

Figure 4. Room temperature IrG1 and DDIrG1 hole mobility as a function of the square root of the electric field.

where σ and Σ are the two central parameters of the disorder formalism; σ is the energy width of the hopping site manifold, and Σ is the positional disorder due to a distribution of intersite distances; C is a constant and $\hat{\sigma} = \sigma / kT$. Equation 1 predicts a Poole–Frenkel (PF) like electric field dependence for a given temperature. Therefore, we plotted mobility against $E^{1/2}$ at each temperature, as shown in Figure 6. The experimental data of Figure 6 are well described by Equation 1 for external electric field $E \geq 1 \times 10^5$ V cm^{-1} ($E^{1/2} > 300$ (V cm^{-1})$^{1/2}$).

The energetic disorder parameter (σ) has been derived from the temperature dependence of the minimum of the mobility, as representative of the asymptotic $\mu(E = 0)$ values:[25–27]

$$\mu_{(E=0)} = \mu_0 \exp\left(-(T_0/T)^2\right) \quad (2)$$

where μ_0 is the mobility at infinite temperature and T_0 is the characteristic temperature of the material investigated. By

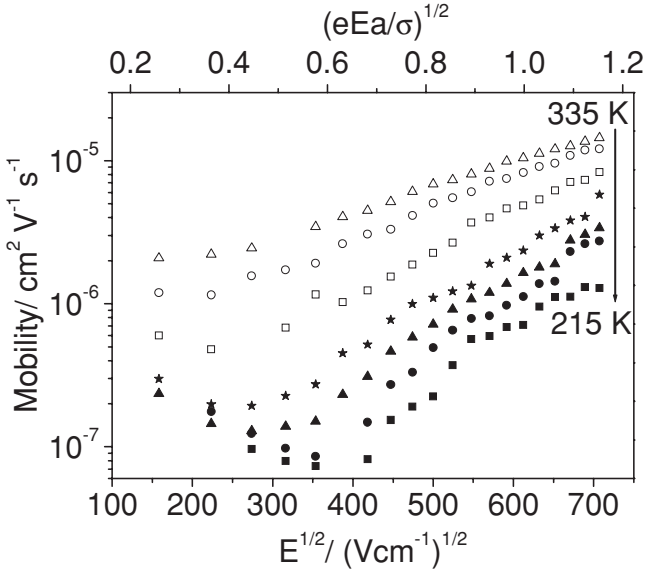

Figure 6. Electric field dependence of mobility of DDIrG1 at temperatures from 215 K to 335 K at intervals of 20 K.

© 2012 WILEY-VCH Verlag GmbH & Co. KGaA, Weinheim

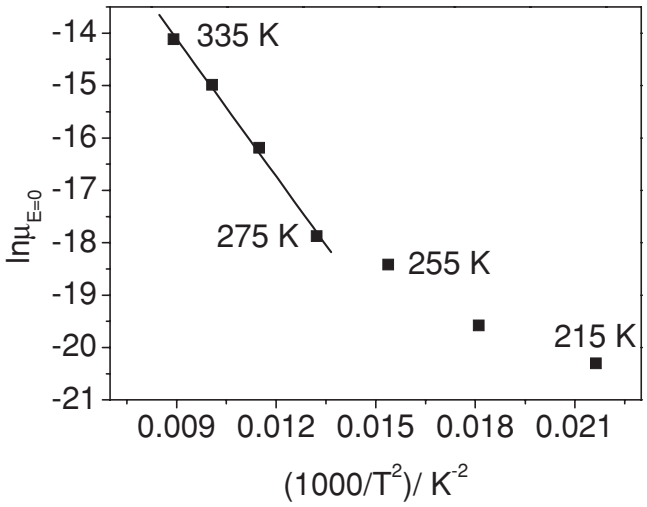

Figure 7. DDIrG1 zero-field mobilities obtained for the various temperatures against $1/T^2$.

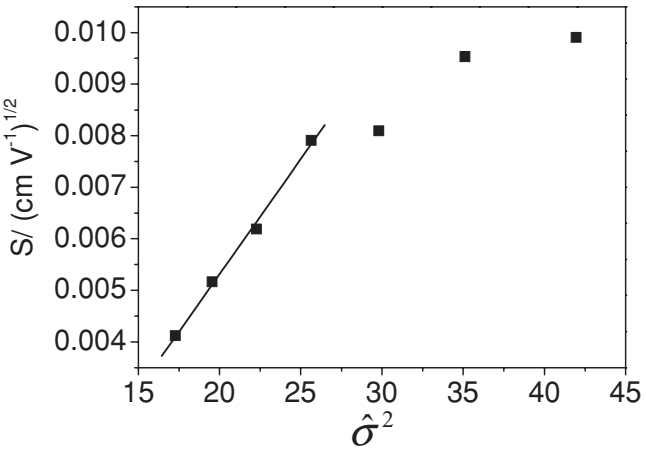

Figure 8. The slope, S, of the data in Figure 6 at different temperatures is plotted against $\hat{\sigma}^2$ to obtain the positional disorder parameter, Σ. The solid line is a fit to the Gaussian disorder model in the region of non-dispersive transport.

plotting $\ln\mu(E = 0)$ against $1/T^2$, as shown in **Figure 7**, and fitting in the range 335 K to 275 K, we can deduce T_0 from the slope to be 750 K for DDIrG1, and μ_0 from the intercept with the y-axis to be 3.4×10^{-4} cm^2 V^{-1} s^{-1}. The width of the Gaussian density of states (DOS) is related to T_0 through the relation, $T_0 = 2\sigma/3k$, where k is the Boltzmann constant. Hence, given a value of $T_0 = 750$ K, the width of the density of states σ was found to be 96 meV.

The change in slope for the data in Figure 7 below 275 K is attributed to the onset of the non-dispersive to dispersive transition (ND–D).[21] This can be clearly seen in the shape of the photocurrent transients as a function of temperature (see Figure 5). As the temperature is decreased, the photocurrent plateau becomes less distinct and disappears below 275 K. The temperature dependence of the mobility is expected to change at the non-dispersive to dispersive transition temperature T_c according to Equation 3

$$(\sigma/kT_c)^2 = 44.8 + 6.7\log L \tag{3}$$

where L is the thickness of the sample in centimetres.[21,28] For a film of thickness 400 nm and $\sigma = 96$ meV, the onset of the ND–D transition should occur at 285 K according to Equation 3, which is similar to that observed experimentally.

The value of Σ was determined by plotting the slope S of the field dependence of the mobility for various temperatures against $\hat{\sigma}^2$. The slopes (S) for each temperature range are determined by fitting the experimental data of Figure 6 for an electric field range $E^{1/2} > 300$ (V cm^{-1})$^{1/2}$, that is in the region where mobility shows a Poole–Frenkel-like electric field dependence. The result is shown in **Figure 8**, and by fitting the data points for the non-dispersive regime of charge transport[21] (275–335 K), we extract Σ from the intercept with the x-axis and C from the slope. This analysis yielded a positional disorder parameter Σ of 2.3 and a value for C of 6.8×10^{-4} (cm V^{-1})$^{1/2}$.

2.2. Correlated Disorder Model

It has been reported that long-range correlations due to charge-dipole interactions exist in disordered organic semiconductors.[22,29] In the GDM, the correlation is not taken into account and thus in order to consider the effects of charge-dipole interactions on charge transport, Novikov et al.[22] have developed a 3D CDM and proposed the following empirical relation to describe charge transport in a correlated disordered material:

$$\mu = \mu_0 \exp\left[-\left(\frac{3\hat{\sigma}_{CDM}}{5}\right)^2 + C_0\left(\hat{\sigma}_d^{3/2} - \Gamma\right)\sqrt{\frac{eaE}{\sigma_d}}\right] \tag{4}$$

In Equation 4 σ_{CDM} denotes the total energetic disorder such as $\sigma_{CDM}^2 = \sigma_d^2 + \sigma_{vdw}^2$, where σ_d is the dipolar component of the disorder and σ_{vdw} is the contribution due to non dipolar disorder (van der Waals). μ_0 has the same meaning as before, C_0 and Γ are constants, and a is the average hopping distance between two adjacent sites. The major difference between the GDM and the CDM is that the latter does not include any spatial disorder.

σ_{CDM} and μ_0 have been deduced by using the same fitting parameters obtained from Figure 7 for the GDM and then using Equation 2, with the only difference that in this case $T_0 = 3\sigma/5k$. Hence, μ_0 has the same value as in the GDM and the value of σ_{CDM} was found to be 107 meV.

We have recently reported neutron reflectivity measurements for a family of iridium(III) complex-cored dendrimers[30] that have allowed us to measure the effective volume and hence diameter of DDIrG1. The effective diameter in the solid state was determined to be 22.6 Å. For conjugated dendrimers such as those studied here, in which the dendron has a wider energy gap than the core, charge resides on the core and charge transport is by hopping between the cores.[14,31,32] Thus we can assume that the average inter-site separation for DDIrG1 is a = 22.6 Å. Hence, C_0 and Γ can be easily determined by plotting the slope (S) of mobility at the different temperatures obtained from Figure 6 against $(\sigma/kT)^{3/2}$. The result is shown in **Figure 9** for the temperature range 215–335 K. We fit the data points in the temperature range 275–335 K, because this is the non-dispersive regime of charge transport, and extract C_0 from the slope and Γ from the intercept with the x-axis. This analysis yielded a value of 1 for C_0 and of 4.45 for Γ.

© 2012 WILEY-VCH Verlag GmbH & Co. KGaA, Weinheim

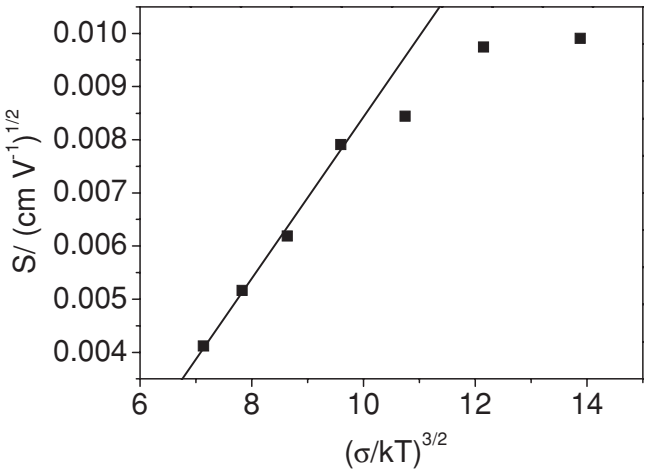

Figure 9. The slope, S, of the data in Figure 6 at different temperatures is plotted against $(\sigma/kT)^{3/2}$ to obtain C_0 and Γ. The solid line is a fit over the non-dispersive region to the CDM.

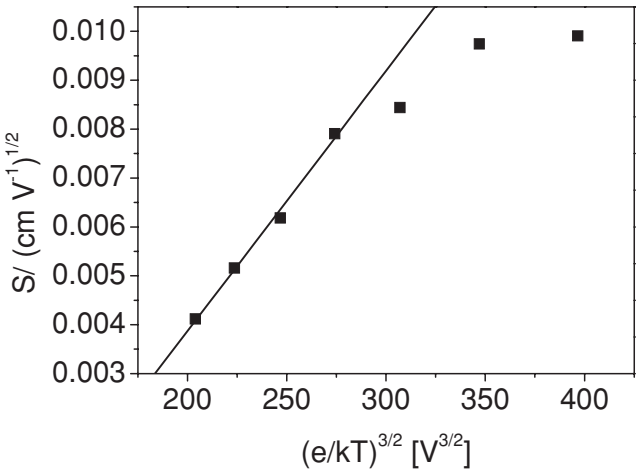

Figure 10. The slope, *S*, of the data in Figure 6 at different temperatures is plotted against $(e/kT)^{3/2}$ to obtain the energetic disorder parameter (σ_{pCDM}) and the constant Γ. The solid line is a fit over the non-dispersive region to the polaronic CDM.

2.3. Correlated Disorder Model with Polaron Effects

Although Equations 1 and 4 can be used to analyze TOF data, recent theoretical work[23] has cast doubt on whether the σ extracted from the experiment using Equations 1 and 4 represents the actual width of the full DOS. Here, we report the first application of incorporating the inter-site correlation and polaron effects to explain the charge transport mechanism in dendrimer films. We analyze the field and temperature dependent mobility data using the model proposed by Parris and co-workers[23] based on the small polaron motion in a correlated disorder landscape. Mobility values from Figure 6 were fitted to Equation 5 to determine the width of the DOS in the polaronic CDM model, σ_{pCDM}, μ_0, E_a, Γ:

$$\mu(T, E) = \mu_0 \exp\left(-\frac{E_a}{kT}\right) \exp - \left(\frac{3\hat{\sigma}_{pCDM}}{5}\right)^2 \exp\left[C_0\left(\hat{\sigma}_{pCDM}^{3/2} - \Gamma\right)\sqrt{\frac{eaE}{\sigma_{pCDM}}}\right] \quad (5)$$

In a similar way to the GDM and CDM, Equation 5 predicts a PF-like behavior, where σ_{pCDM}, μ_0 and a have the same meanings as before and C_0 and Γ are constants.

The values of σ_{pCDM} and Γ have been determined by plotting the slope (S) of the mobility field dependence at the different temperatures obtained from Figure 6 against $(e/kT)^{3/2}$. The result is shown in **Figure 10** for the temperature range 215–335 K, and by fitting the data points for the temperature range 275–335 K, σ_{pCDM} and Γ are extracted. Assuming the same value of C_0 determined by the CDM, this analysis yielded an energetic disorder of 112 meV and a Γ value of 4.76.

In order to determine the last unknown parameters (E_a and μ_0), we consider mobility at zero field. Equation 5 simplifies to the following:

$$\mu(T, E = 0) = \mu_0 \exp\left(-\frac{E_a}{kT}\right) \exp - \left(\frac{3\hat{\sigma}_{pCDM}}{5}\right)^2 \quad (6)$$

By plotting the zero field mobility against T^{-1} we find E_a to be –20 ± 30 meV (graph not shown). Clearly a negative value of the activation energy would be unphysical, and even the positive value at the upper end of the error range is unreasonable as it is much smaller than the energetic disorder (σ_{pCDM}).

2.4. Short-Range Correlated Gaussian Disorder Model

Although the GDM explains the field and temperature dependence of a wide range of organic materials,[33–36] its PF-like mobility dependence is only valid over a short range of electric fields, and for relatively high electric fields ($E \geq 3 \times 10^5$ V cm^{-1}).[22] In the last decade starting from the original GDM many authors[22,29,37,38] have reported that introducing a long-range correlation between hopping sites (CDM and polaronic CDM) produces the expected PF-like dependence over a wider range of electric fields. In these models the correlation arises from interactions between charges and randomly oriented permanent dipoles.[29]

Here we apply the model of Tonezer and Freire[24] to our TOF mobility measurements. The model is based on Gaussian distribution of DOS, where the only source of the hopping site energies is given by the interaction of the charge in the site with the surrounding induced dipoles (short-range correlation). This model predicts a PF-like mobility dependence over a significant range of fields and give the following expression for the mobility:[24]

$$\mu = \mu_0(T) \exp\left[\left(1.6\frac{\alpha e^e}{2kTa^4} - 2.9\right)\sqrt{\frac{eEa}{kT}}\right] \quad (7)$$

where α is the isotropic polarizability of all sites and the other parameters have the same meaning as before.

Figure 6 shows the logarithm of the mobility as function of the square root of dimensionless field $(\sqrt{eEa/\sigma})$ for different temperature values. Our experimental data show a PF mobility

© 2012 WILEY-VCH Verlag GmbH & Co. KGaA, Weinheim

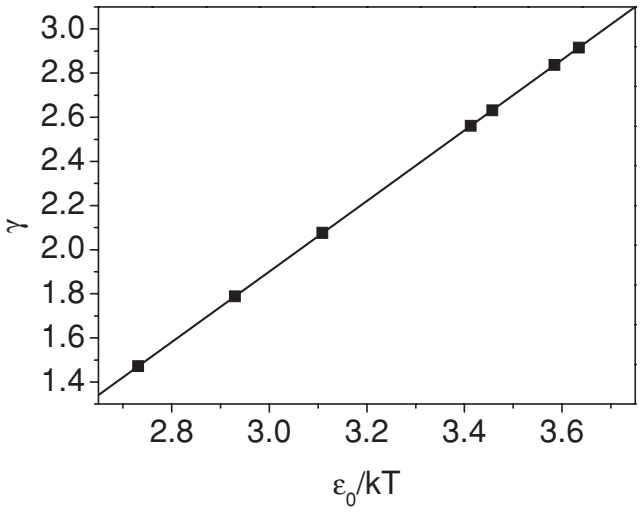

Figure 11. The dimensionless parameter γ against ε_0/kT.

dependence in the range of $0.5 < \sqrt{eEa/\sigma} < 1.15$. The energetic disorder parameter has been defined as $\sigma = \sqrt{1.16}\varepsilon_0$, where ε_0 is the energy scale of the polarization energy and is given by $\varepsilon_0 = e^2\alpha/2a^4$. ε_0 has been determined measuring the field dependence (slope) of the mobility from Figure 6. In fact from Equation 7, the slope (γ) is related to ε_0 by the following equation:

$$\gamma = 1.6\frac{\alpha e^2}{2kTa^4} - 2.9 = 1.6\frac{\varepsilon_0}{kT} - 2.9 \quad (8)$$

Figure 11 shows a plot of γ against ε_0/kT, and the solid line is the linear fit to the experimental data using Equation 8. This fit gives a value of 85 meV for the energetic disorder parameter σ.

3. Discussion

We first consider the nature of charge transport in DDIrG1. The shape of the current transient for DDIrG1 signifies that hole transport is highly non-dispersive in this dendrimer at room temperature, in contrast to the previously reported room temperature measurements for the singly dendronised IrG1 and its second generation analogue (IrG2).[32] That is, the current transient indicates that films of DDIrG1 are less disordered than those of the first- and second-generation singly dendronised materials IrG1 and IrG2.[8] Non-dispersive transients in more ordered films have also been observed in conjugated polymers. Inigo and co-workers[39] reported a non-dispersive photocurrent transient in a low defect density MEH-PPV sample with an energetic and positional disorder parameters of $\sigma = 76$ meV and $\Gamma = 1.48$; meanwhile for a higher defect density sample a dispersive photocurrent transient was observed together with higher values of σ (82 meV) and of Γ (4.5) for the same material. A similar result but on a different conjugated polymer (PFO) has been reported by Kreouzis and co-workers.[40] They found a reduction in the energetic disorder from 95 meV down to 73 meV upon annealing the sample that indicates that the film becomes more ordered after annealing. This transition is clearly manifested from a highly dispersive photocurrent transient for the non annealed PFO sample to a clearly non-dispersive behaviour for the annealed one. Laquai and co-workers[41] report for a polyspirobifluorene polymers that increasing the disorder in their materials leads to a higher dispersion of TOF transients.

We have investigated whether the GDM can explain the variation of photocurrent transients with temperature and field for DDIrG1. Our value of σ of 96 meV, yields an energetic disorder of $\hat{\sigma} = 3.7$ at room temperature. This value is within the estimated values from Monte Carlo simulation for a non-dispersive photocurrent transient, where $\hat{\sigma} \leq 3.5 - 4$ is expected for non-dispersive charge transport behaviour.[21]

The temperature transition from non-dispersive to dispersive charge transport behaviour means that below this temperature (see Figure 5), the carriers will cross the sample without relaxing to their mean energy. DDIrG1 exhibits non-dispersive transport at temperatures down to 275 K, which is lower than the transition temperature of 293 K for IrG1. The theoretical transition temperature determined from Equation 3 of 285 K is very close to that determined from experiment (275 K).

We have discussed so far the good agreement of our experimental data with PF-like behaviour for electric fields higher than 1×10^5 V cm^{-1} ($E^{1/2} > 300$ (Vcm^{-1})$^{1/2}$); another important feature of the data in Figure 6 is the negative field dependence of the mobility at low fields. This negative field dependence has been observed in a wide range of organic materials.[42–44] This is due to the positional disorder, because faster routes made up of more favourable charge-transporting site, with part of their path going against the field are forbidden as the field increases. These results are in very good agreement with the GDM.[21,28]

Different theoretical models have been used to explain charge transport in molecularly doped polymers (MDP),[29,45] polymers,[46–48] and organic glasses.[22] For instance, recently Kreouzis and co-workers[40] have reported a detailed study regarding the consistency of their PFO TOF experimental data to the polaronic CDM. Another recent development is the possibility of modelling the mobility of an organic material starting from the consideration of the atomic structure of the material as recently reported by Nelson et al.[49] and Vukmirovic et al.[50,51]

To characterize the CDM we measured the energetic disorder parameter in a similar way to the GDM and we found σ_{CDM} = 107 meV. The σ_{CDM} is slightly higher than σ_{GDM} but this is consistent with the results reported by others on a range of materials,[52,53] suggesting that the charge–dipole interaction is a stronger source of energetic disorder. For a direct comparison with the GDM, we calculated $\hat{\sigma}_{CDM}$ and the transition temperature using Equation 3. This yielded $\hat{\sigma}_{CDM} = 4.2$ and $T_c = 317$ K. This is substantially higher than the experimental value of 275 K, and the energetic disorder parameter fails to satisfy the relation $\hat{\sigma}_{CDM} \leq 3.5$.

The coefficient Γ is analogous to the positional disorder parameter Σ^2 of Equation 1, but in the CDM it is supposed to be a constant value. Our estimated value of Γ of 4.45 is more than double the value of 2 calculated by Novikov et al.[22] This discrepancy between experimental and simulation value of Γ is consistent with previous reported results on an organic glass material[22] and polymers,[54] and it has been ascribed to the

© 2012 WILEY-VCH Verlag GmbH & Co. KGaA, Weinheim

fact that the CDM does not take into account any positional disorder.

Hence the introduction of inter-site correlations does not improve the agreement between experimental and theoretical data, at least for films of DDIrG1. The next step in the analysis was to use the polaronic CDM. A critical test for a polaron activated contribution to temperature-dependent transport is provided by the comparison between the temperature-dependence of the carrier mobility and the onset of dispersion of TOF signals at lower temperature.[21] If both sets of data are consistent, the polaronic contribution must be negligible compared with disorder effects. If, on the other hand, the onset of dispersion starts at a lower temperature, that is, smaller $\hat{\sigma}$, this provides a handle for separating disorder from polaronic effects. We have already seen from the experimental data that the transition temperature T_c is lower than that predicted by theory, showing that for DDIrG1 the activation energy of transport could then be the sum of disorder and polaron contributions.[21]

The polaronic CDM analysis yielded an energetic disorder parameter σ_{pCDM} = 112 meV and a Γ value of 4.76. The value of the energetic disorder is even higher than in the CDM, which leads to a $\hat{\sigma}_{pCDM}$ value of 4.4 and once again the expected relation $\hat{\sigma} \leq 3.5$ for non-dispersive charge transport behaviour[21] is not satisfied. This value of the energetic disorder parameter leads to (via equation 6) a negative value of the polaron activation energy (E_a). This is unphysical and clear evidence that the polaronic CDM does not fit our experimental data.

Our results suggest that the analysis of the experimental data carried out within the polaronic CDM does not work well for dendrimers even though it did work for poly(9,9-di-*n*-octylfluorene).[40] However, it is important to remember that polymers are pseudo one-dimensional whereas the dendrimers in this study are three-dimensional.

The last model to be discussed is the one based on short range correlation. This model has been developed quite recently and to the best of our knowledge so far no TOF experimental data have been analyzed using it. It predicts a PF-like dependence of the mobility in the range $0.5 < \sqrt{eEa/\sigma} < 1.1$, that is in very good agreement with our experimental data. The value of the energetic disorder parameter of 85 meV, gives a room temperature value of $\hat{\sigma}$ of 3.3, thus satisfying the relation $\hat{\sigma} \leq 3.5$, which is expected for non dispersive charge transport behaviour.

The good fit of this model to our TOF experimental results could be due to the fact that this model is based on site locations that are supposed to be the center of hard spheres randomly distributed. That is a scenario similar to our system, i.e. spherical shape molecules[30] whose hopping site is at the center of the molecule itself (chromophore).

We finally consider how the field dependent mobility of the first generation doubly dendronised dendrimer (DDIrG1) compares with the first generation mono-dendronised material (IrG1). Both dendrimers show similar mobility, which is double that of the second-generation mono-dendronised dendrimer (IrG2).[32]

We have recently reported[30] that the average volumes occupied by IrG1 and IrG2 in a film are 3100 and 6000 Å^3, respectively. These volumes correspond to diameters of 18.1 and 22.5 Å for IrG1 and IrG2. Hence it is clear that increasing the distance between the electroactive chromophore in moving from IrG1 to IrG2 gives rise to a decreased mobility. Given that the diameter for DDIrG1 is similar to IrG2 and larger than IrG1 it is very interesting that the mobility of DDIrG1 is almost double that of IrG2. For the doubly dendronised dendrimer dendrons on both (hetero)aromatic units of the ligands of the complex will give rise to a more spherical shape[30] and hence a narrower distribution of chromophore spacing. This would mean that the DDIrG1 is less disordered in the solid state than IrG1. This is consistent with the clearly non-dispersive photocurrent transient of DDIrG1 mentioned above and its lower energetic disorder (σ = 96 meV) compared to the reported value for IrG1 (σ = 103 meV).[32] In a previous dendrimer family having the same iridium based chromophore, but carbazole containing dendrons and 9,9-di-*n*-propylfluorenyl surface groups, we also found that a less disordered material has higher mobility and a clearly non-dispersive photocurrent transient when compared to a more disordered one.[8] Similar effects have been seen in polymers. For example, regioregular poly(3-*n*-hexylthiophene) shows a higher mobility than that of regiorandom material.[55]

4. Conclusions

TOF mobility measurements have been used to study the influence of dendrimer structure on charge transport. The data were analysed using four models: the Gaussian disorder model (GDM), the correlated disorder model (CDM), the polaronic correlated disorder model (polaronic CDM), and the short range correlated Gaussian disorder model (short CDM).

The experimental results analyzed within the GDM show a very good agreement between the calculated main parameters such as the energetic disorder $\hat{\sigma}$, the transition temperature (T_c) and the expected simulation values. Furthermore, the non-dispersive charge transport nature of DDIrG1 has allowed investigating its charge transport behaviour in a wide range of temperature and electric fields showing a very good match in the description of the non-dispersive to dispersive transition within the Gaussian disorder model.

The introduction of spatial correlation in site energies has led to the so-called CDM, which has been applied to our experimental data. The calculated parameters differ in value to the ones reported by simulation,[22] which arises because the CDM does not take into account any positional disorder. This is consistent with previous reported results where the presence of the positional disorder due to the amorphous nature of the organic material plays an important role and clearly must be taken into account in a theoretical model describing charge transport.

We apply for the first time the polaronic CDM into the analysis of the experimental TOF measurements in conjugated dendrimers. Despite the introduction of both energy correlation and the polaronic hopping effect, the experimental results analyzed within the polaronic CDM leads to an unphysical value of the activation energy. This means that there is no contribution to the activation energy of charge transport from polaronic effects. This is consistent with our results because of the good agreement between the simulated (in the GDM) and the experimental value of the non-dispersive to dispersive transition temperature.

© 2012 WILEY-VCH Verlag GmbH & Co. KGaA, Weinheim

Finally we report, to the best of our knowledge, also the first attempt of fitting TOF experimental data to a recently developed model based on a spatially disordered system where the site energies are given by the interaction of a charge with the induced dipoles in the surrounding sites. This short CDM model describes, better than the previous two correlated models (CDM and polaronic CDM), our experimental TOF results. Its good description of the dendrimer studied here suggests it would be worthwhile to investigate its application to TOF measurements of other organic semiconductors.

Furthermore we found that the first generation doubly dendronised (DDIrG1) and mono-dendronised dendrimer (IrG1) have the same mobility, which is double that of the second generation singly dendronised dendrimer (IrG2).[32] The improvement in charge transport is directly related to the reduced disorder in the DDIrG1 film. Hence, the enhanced film PLQY of DDIrG1 is not gained at the expense of charge transport, showing that we were able to improve the PL properties of the core without inhibiting its charge transport properties. Our results show that it is not only the size, but also the shape of the macromolecule which determines the mobility. We show that a doubly dendronised configuration is an efficient way of reducing molecular interactions that cause the quenching of the luminescence, whilst maintaining good mobility values.

5. Experimental Section

Charge transport was measured by the charge-generation layer TOF technique. Solutions of IrG1 and DDIrG1 were made with concentrations of 45–50 mg mL^{-1} in chloroform. Films were made by spin-coating onto an indium tin oxide (ITO) substrate at speeds of 800–1000 rpm to obtain films of about 400 nm thickness. The samples were then transferred to an evaporator where under high vacuum a 10 nm layer of a perylene dye (Lumogen Red) followed by 100 nm of aluminum were deposited through a shadow mask to define the active area of approximately 6 mm^2.

The sample was mounted in a vacuum cryostat allowing control of the sample temperature both above and below room temperature. Device testing was undertaken by exciting the charge generation layer through the ITO and dendrimer layer. Charge carriers were generated within the perylene layer by excitation from a 500 ps pulse of a dye laser at a wavelength of 580 nm. At this excitation wavelength the dendrimers are completely transparent (see Figure 2) and Lumogen Red has its peak of absorption.[56] The total photogenerated charge was kept small enough to avoid space charge effects, usually around 2–3% CV, where C is the capacitance of the device and V the applied voltage. The electronic time response of the measurement circuit ($\tau = RC$) was always selected to be much smaller than the transit time, $\tau << t_{tr}$.

The aluminium electrode was biased positively and the photocurrent signal detected from the ITO (see Figure 2, inset). Hole mobilities, μ, were deduced from the transit times, t_{tr}, via the relation $\mu = d^2/Vt_{tr}$, where d is the film thickness.

Acknowledgements

We are grateful to the UK Engineering and Physical Sciences Research Council for financial support. Professor Paul Burn is the recipient of an Australian Research Council Federation Fellowship (Project FF0668728).

Received: July 27, 2011
Published online: October 19, 2011

[1] T. Swager, *Nat. Mater.* **2002**, *1*, 151.
[2] I. F. Perepichka, D. F. Perepichka, H. Meng, F. Wudl, *Adv. Mater.* **2005**, *17*, 2281.
[3] E. B. Namdas, A. Ruseckas, I. D. W. Samuel, S.-C. Lo, P. L. Burn, *Appl. Phys. Lett.* **2005**, *86*, 091104.
[4] J.-C. Ribierre, A. Ruseckas, I. D. W. Samuel, H. S. Barcena, P. L. Burn, *J. Chem. Phys.* **2008**, *28*, 204703.
[5] S.-C. Lo, R. E. Harding, E. Brightman, P. L. Burn, I. D. W. Samuel, *J. Mater. Chem.* **2009**, *19*, 3213.
[6] M. Pope, C. E. Swenberg, *Electronic Processes in Organic Crystals*, Oxford University Press, Oxford, UK **1982**.
[7] B. K. Yap, R. Xia, M. Campoy-Quiles, P. N. Stavrinou, D. D. C. Bradley, *Nat. Mater.* **2008**, *7*, 376.
[8] S. Gambino, S. G. Stevenson, K. A. Knights, P. L. Burn, I. D. W. Samuel, *Adv. Funct. Mater.* **2009**, *19*, 317.
[9] H. Kim, N. Schulte, G. Zhou, K. Müllen, F. Laquai, *Adv. Mater.* **2011**, *23*, 894.
[10] S. Z. Bisri, T. Takenobu, Y. Yomogida, H. Shimotani, T. Yamao, S. Hotta, Y. Iwasa, *Adv. Funct. Mater.* **2009**, *19*, 1728.
[11] S.-C. Lo, P. L. Burn, *Chem. Rev.* **2007**, *107*, 1097.
[12] P. L. Burn, S.-C. Lo, I. D. W. Samuel, *Adv. Mater.* **2007**, *19*, 1675.
[13] N. C. Cumpstey, R. N. Bera, P. L. Burn, I. D. W. Samuel, *Macromolecules* **2005**, *38*, 9564.
[14] M. Halim, J. N. G. Pillow, I. D. W. Samuel, P. L. Burn, *Adv. Mater.* **1999**, *11*, 371.
[15] J. M. Lupton, I. D. W. Samuel, R. Beavington, P. L. Burn, H. Bässler, *Adv. Mater.* **2001**, *13*, 258.
[16] S.-C. Lo, R. E. Harding, C. P. Shipley, S. G. Stevenson, P. L. Burn, I. D. W. Samuel, *J. Am. Chem. Soc.* **2009**, *131*, 16681.
[17] S.-C. Lo, N. A. H. Male, J. P. J. Markham, S. W. Magennis, P. L. Burn, O. V. Salata, I. D. W. Samuel, *Adv. Mater.* **2002**, *14*, 975.
[18] E. J. Wren, X. Wang, A. Farlow, S.-C. Lo, P. L. Burn, P. Meredith, *Org. Lett.* **2010**, *12*, 4338.
[19] J.-C. Ribierre, S. Stevenson, I. D. W. Samuel, S. V. Staton, P. L. Burn, *J. Display Technol.* **2007**, *3*, 233.
[20] S.-C. Lo, T. D. Anthopoulos, E. B. Namdas, P. L. Burn, I. D. W. Samuel, *Adv. Mater.* **2005**, *17*, 1945.
[21] H. Bässler, *Phys. Status Solidi B* **1993**, *175*, 15.
[22] S. V. Novikov, D. H. Dunlap, V. M. Kenkre, P. E. Parris, A. V. Vannikov, *Phys. Rev. Lett.* **1998**, *81*, 4472.
[23] P. E. Parris, V. M. Kenkre, D. H. Dunlap, *Phys. Rev. Lett.* **2001**, *87*, 126601.
[24] C. Tonezer, J. A. Freire, *J. Chem. Phys.* **2010**, *133*, 214101.
[25] P. M. Borsenberger, R. Richert, H. Bässler, *J. Chem. Phys.* **1991**, *94*, 5447.
[26] P. M. Borsenberger, L. T. Pautmeier, H. Bässler, *Phys. Rev. B* **1992**, *46*, 12145.
[27] P. M. Borsenberger, R. Richert, H. Bässler, *Phys. Rev. B* **1993**, *47*, 4289.
[28] P. M. Borsenberger, D. S. Weiss, *Organic Photoreceptors for Xerography*, M. Dekker, New York **1998**.
[29] D. H. Dunlap, P. E. Parris, V. M. Kenkre, *Phys. Rev. Lett.* **1996**, *77*, 542.
[30] S. V. Vickers, H. Barcena, K. A. Knights, R. K. Thomas, J.-C. Ribierre, S. Gambino, I. D. W. Samuel, P. L. Burn, G. Fragneto, *Appl. Phys. Lett.* **2010**, *96*, 263302.
[31] J. M. Lupton, I. D.W. Samuel, R. Beavington, M. J. Frampton, P. L. Burn, H. Bässler, *Phys. Rev. B* **2001**, *63*, 155206.
[32] J. P. J. Markham, I. D. W. Samuel, S.-C. Lo, P. L. Burn, M. Weiter, H. Bässler, *J. Appl. Phys.* **2004**, *95*, 438.
[33] H. H. Fong, K. C. Lun, S. K. So, *Chem. Phys. Lett.* **2002**, *353*, 407.
[34] A. R. Inigo, H. C. Chiu, W. Fann, Y. S. Huang, U. S. Jeng, T. L. Lin, C. H. Hsu, K. Y. Peng, S. A. Chen, *Phys. Rev. B* **2004**, *69*, 075201.
[35] M. Redecker, D. D. C. Bradley, M. Inbasekaran, W. W. Wu, E. P. Woo, *Adv. Mater.* **1999**, *11*, 241.

© 2012 WILEY-VCH Verlag GmbH & Co. KGaA, Weinheim

[36] F. Laquai, G. Wegner, C. Im, H. Bässler, S. Heun, *J. Appl. Phys.* **2006**, *99*, 033710.
[37] A. Dieckmann, H. Bässler, P.M. Borsenberger, *J. Chem. Phys.* **1993**, *99*, 8136.
[38] Y. N. Garstein, E. M. Conwell, *Chem. Phys. Lett*. **1995**, *245*, 351.
[39] A. R. Inigo, H.-C. Chiu, W. Fann, Y.-S. Huang, U. S. Jeng, C. H. Hsu, K.-Y. Peng, S.-A. Chen, *Synth. Metal.* **2003**, *139*, 581.
[40] T. Kreouzis, D. Poplavskyy, S. M. Tuladhar, M. Campoy-Quiles, J. Nelson, A. J. Campbell, D. D. C. Bradley, *Phys. Rev. B* **2006**, *73*, 235201.
[41] F. Laquai, G. Wegner, C. Im, H. Bässler, S. Heun, *J. Appl. Phys.* **2006**, *99*, 023712.
[42] A. Peled, L. B. Schein, *Chem. Phys. Lett.* **1988**, *153*, 422.
[43] H. Kageyama, K. Ohnishi, S. Nomura, Y. Shirota, *Chem. Phys. Lett.* **1997**, *277*, 137.
[44] P. M. Borsenberger, L. Pautmeier, H. Bässler, *J. Chem. Phys.* **1991**, *94*, 5447.
[45] L. B. Schein, D. Glatz, J. C. Scott, *Phys. Rev. Lett.* **1990**, *65*, 472.
[46] S. V. Rakhmanova, E. M. Conwell, *Synth. Met.* **2001**,*116*, 389.
[47] C. Tanase, E. J. Meijer, P. W. M. Blom, D. M. de Leeuw, *Phys. Rev. Lett.* **2003**, *91*, 216601.
[48] C. Tanase, P. W. M. Blom, D. M. de Leeuw, E. J. Meijer, *Phys. Staus. Solidi A* **2004**, *201*, 1236.
[49] J. Nelson, J. J. Kwiatkowski, J. Kirkpatrick, J. M. Frost, *Acc. Chem. Res.* **2009**, *42*, 1768.
[50] N. Vukmirović, L.-W. Wang, *Phys. Rev. B* **2010**, *81*, 035210.
[51] N. Vukmirović, L.-W. Wang, *Nano Lett.* **2009**, *9*, 3996.
[52] C. Vijila, A. Pivrikas, H. Chun, C. Zhikuan, R. Osterbacka, C. S. Jin, *Org. Electron.* **2007**, *8*, 8.
[53] M. Parameswaran, G. Balaji, T. M. Jin, C. Vijila, S. Vadukumpully, Z. Furong, S. Valiyaveettil, *Org. Electron.* **2009**, *10*, 1534.
[54] R. U. A. Khan, D. Poplavskyy, T. Kreouzis, D. D. C. Bradley, *Phys. Rev. B* **2007**, *75*, 035215.
[55] H. Sirringhaus, P. J. Brown, R. H. Friend, M. M. Nielsen, K. Bechgaard, B. M. W. Langeveld-Voss, A. J. H. Spiering, R. A. J. Janssen, E. W. Meijer, P. Herwig, D. M. De Leeuw, *Nature* **1999**, *401*, 685.
[56] S. Gambino, I. D. W. Samuel, H. Barcena, P. L. Burn, *Org. Electron.* **2008**, *9*, 220.

© 2012 WILEY-VCH Verlag GmbH & Co. KGaA, Weinheim